Journal of Achievements in Materials and Manufacturing Engineering
VOLUME 19
ISSUE 2
December
2006

Modified 9% Cr steels for advanced power generation: microstructure and properties

A. Czyrska-Filemonowicz [a], A. Zielińska-Lipiec [a], P.J. Ennis [b]
[a] Faculty of Metals Engineering and Industrial Computer Science,
AGH University of Science and Technology (AGH-UST)
Al. Mickiewicza 30, 30-059 Kraków, Poland
[b] Institute for Materials and Processes in Energy Systems 2
Research Centre Jülich (FZJ), 52425 Jülich, Germany
* Corresponding author: E-mail address:

Received in revised form 15.07.2006; accepted in final form 30.10.2006

Methodology of research

ABSTRACT

Purpose: The 9-10%Cr steels developed for advanced power stations, P91, P92 and E911, have been investigated.
Design/methodology/approach: Quantitative microstructural investigations (sub-grain width, dislocation density, particle size distribution and their chemical compositions) have been carried out using analytical transmission electron microscopy.
Findings: Comparison of the microstructural parameters of three 9%Cr steels mentioned above and a correlation with different creep rupture behaviour are presented. The results show that in the first 3000 h of creep exposure at 600 and 650°C, there was a rapid reduction in the dislocation density and an increase in a tempered martensite sub-grain width. During long-term creep deformation, the $M_{23}C_6$ carbides coarsened, while the MX precipitates exhibited insignificant change in size. Large particles of Laves phase, $Fe_2(Mo,W)$ were also precipitated.
Practical implications: The microstructural changes were reflected in the results of the creep tests. The high creep strength that can be achieved in the investigated steels enables these steels to be considered for applications in advanced power plants operating at steam temperatures above 600°C.
Originality/value: Microstructural parameters deciding creep rupture properties of the examined steel have been determined.
Keywords: Martensite steel; Creep; Microstructure; Transmission electron microscopy (TEM)

1. Introduction

The increase in the thermal efficiency of fossil fuel fired steam power plant that can be achieved by increasing the steam temperature and pressure has provided the incentive for the development of the 9% chromium steels towards improved creep rupture strength. During the last twenty years, three such steels, P91 (9Cr-1Mo-V-Nb), E911 (9Cr-1Mo-1W-V-Nb) and P92 (9Cr-0.5Mo-1.8W-V-Nb), have been developed to commercial production. P91 was originally developed by the Oak Ridge National Laboratory for application in the fast breeder reactor and has now become a well established steel for power station components [1]. There are extensive and reliable design data available, which allow the 10^5 h rupture strength at 600°C to be confidently specified; P91 is covered by the American standards ASTM 213 and 335. P92 was developed by Nippon Steel in Japan

under the company designation NF616 and a data collection has been issued [2]. The steel is also included in ASTM 335 as P92. The 10^5 h rupture strength is given as 130 MPa, based on the Nippon Steel data. E911 was developed first as a rotor steel in the European COST Round II activities and then as a piping and tubing steel in the COST Round III programmes [3]. Some long-term data are now becoming available. In the present work, the creep rupture behaviour of the three steels has been investigated and the reasons for the observed differences in the stress rupture strengths will be discussed. Standard creep rupture tests have been carried out and the comparison of creep strength has been made by analysis of the secondary creep rates, in addition to the usual stress rupture curves.

The microstructures of selected specimens were examined using transmission electron microscopy (TEM) of thin foils and extraction double replicas. The TEM investigations were carried out to determine the microstructural parameters (sub-grain width, dislocation density, particle size distribution) of the P91, P92 and E911 steels, so that the relationship between microstructure and creep rupture behaviour could be established. Further development of these steels based on quantitative investigations of microstructural stability and on oxidation studies [4] is discussed.

2. Experimental details

The details of the heats investigated are shown in Table 1. Standard creep rupture specimens were machined from the materials and tested at 600-675°C.

From the creep curves at 600 and 650°C, the secondary (steady state) creep rate was determined. The microstructures of the materials in the as received condition were investigated by optical metallography and TEM. The details of the TEM procedures are given in [7, 8].

3. Results and discussion

3.1. Creep behaviour

The stress rupture data determined in this work for the steels P91, E911 and P92 at 600 and 650°C are shown in Figure 1 which is an iso-stress plot of the rupture time against test temperature for an initial stress of 120 MPa. The P9 data were taken from [5]. For the tests of long duration which are still in progress, the rupture life was predicted from the secondary creep rate using the Monkman-Grant equation as described in [6]; the predictions are shown by the open data points in Fig.1. The greatest difference in strength was between P9 and P91 and this demonstrates the considerable strengthening achieved by the addition of small amounts of V and Nb together with the partial substitution of C by N. The additional increase in rupture strength of E911 and P92 over P91 can be attributed to the addition of W. Figure 2 shows the secondary creep rates ($\dot{\varepsilon}_s$) of P91, P92 and E911 plotted against the applied stress (σ). Data taken from published literature are included where available.

Table 1.
Details of test material

	chemical composition, wt%			
element	P9 (specification)	P91	P92	E911
C	0.06 – 0.18	0.10	0.124	0.105
Si	0.10 – 0.85	0.38	0.02	0.20
Mn	0.3 – 0.6	0.46	0.47	0.35
P	< 0.03	0.020	0.011	0.007
S	< 0.03	0.002	0.006	0.003
Cr	8.2 – 9.8	8.10	9.07	9.16
Mo	0.8 – 1.2	0.92	0.46	1.01
W	-	-	1.78	1.00
V	-	0.18	0.19	0.23
Nb	-	0.073	0.063	0.068
B	-	-	0.003	-
N	-	0.049	0.043	0.072
Ni	0.05 – 0.40	0.33	0.06	0.07
Al	< 0.4	0.034	0.002	-
Form and dimensions, mm	-	pipe, ϕ 159, 20 wall thickness	pipe, ϕ 300, 40 wall thickness	flat bar, 100 x 16
Heat treatment	austenitized and tempered	½ h/1050°C + 1 h/750°C, air cooled	2 h/1070°C + 2 h/775°C, air cooled	1 h/1050°C + 1 h/750°C, air cooled
100 000 h stress rupture strength at 600°C, MPa*	32	94	115	110

* values for P9 from [6], P91 from Canonico [7], for P92 from Wachter et al [8], for E911 from Staubli et al [4]

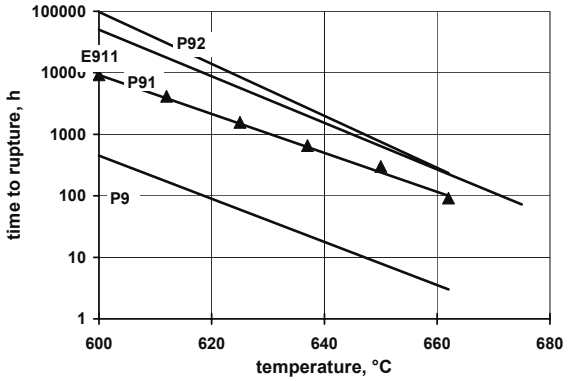

Fig.1. Iso-stress (120 MPa) rupture data for P9, P91, E911 and P92 steels

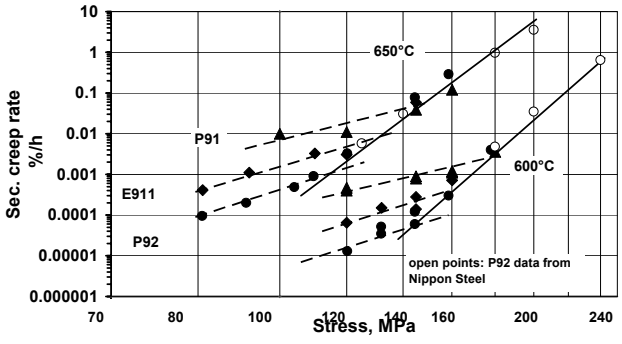

Fig. 2. Secondary creep rates of P91, P92 and E911 at 600 and 650°C plotted as a function of the applied stress

The data for all three steels showed two distinct regions of creep behaviour, which can be described by the Norton equation:

$$\varepsilon_s = k\sigma^n$$

with two different values for the Norton stress exponent n and the constant k. At high stresses, the value of n is around 16 while at lower stresses, the data conform to an n value of 6. The change in n is indicative of a change in the creep strengthening mechanism.
Figure 2 also shows that at high stresses the differences in the secondary creep rates of the three steels were relatively small. In the low stress region, however, the differences between the steels became more pronounced, especially at the higher test temperature.

The microstructures of tested creep specimens were examined in an attempt to correlate the observed change in creep behaviour with the structural characteristics. In the following sections, the microstructural features and their evolution with increasing creep duration will be discussed.

3.2. Microstructural characterization

The microstructure of the 9-10%Cr steels consists of tempered martensite with a high dislocation density and finely distributed carbides, nitrides or carbonitrides. For the application of these materials in steam power plants, the microstructural stability during service is of great importance.

The following structural features are expected to exert an influence on the creep rupture properties of the steels :

- the dislocation density within the martensite laths;
- polygonization conditions of the subgrains;
- fine, uniformly dispersed carbides and carbonitrides within the structure;
- solid solution strengthening of the matrix by elements such as chromium, molybdenum and tungsten;
- formation of intermetallic phases, such as Laves phase.

As received condition

Qualitative TEM investigations showed similar microstructures of tempered martensite for all three steels examined. Figure 3 shows the microstructures of P92 and E911 steels.

Normalization produced a martensitic structure with a high dislocation density within the martensite laths. During tempering, two main processes seemed to be taking place. Firstly, recovery caused the formation of sub-grains and dislocation networks. The creep strength of 9%Cr steels is correlated inversely with the martensite lath width and therefore with the sub-grain size (the original martensite lath boundaries form the sub-grain boundaries). Measurements of the average sub-grain width (w) and of the dislocation density within the sub-grains are presented in Table 2. It can be seen that w is fairly similar in all steels investigated. The small differences in w are connected with different prior austenite grain size. Dislocation densities in P91 and P92 steels are similar; and are higher than in E911 steel.

Table 2.
Dislocation density and a mean sub-grain size of P91, P92 and E911 steels in the as received condition

steel	dislocation density, $m^{-2} \times 10^{14}$	mean sub-grain size, w, μm
P91	7.5 ± 0.8	0.40 ± 0.06
P92	7.9 ± 0.8	0.42 ± 0.09
E911	6.5 ± 0.6	0.50 ± 0.05

Secondly, the precipitation of carbides, carbonitrides and nitrides occurred during tempering. In all three steels examined, the $M_{23}C_6$ carbides containing Cr, Fe, Mo (W) precipitated preferentially on the prior austenite grain boundaries and on the martensite lath boundaries. These precipitates retard the sub-grain growth and therefore increase the strength of the materials.

The important precipitates for the mechanical properties of 9% Cr steels are the fine MX (where M=Nb or V and X=C and/or N). They pin free dislocations in the matrix leading to increasing creep strength of these steels. In P91 steel mainly spheroidal Nb-rich carbonitrides were observed within the martensite laths. In P92 steel three type of MX precipitates were present: fine spheroidal Nb(C,N) and plate-like VN particles as well as some complex "V-wings" Nb(C,N)-VN. The precipitates that formed in E911 were similar.

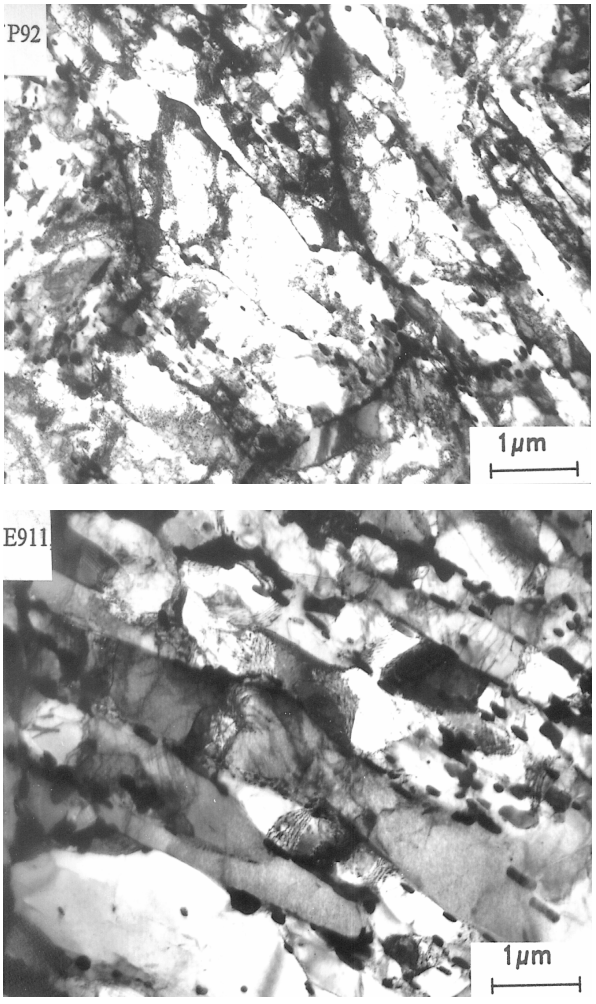

Fig. 3. TEM micrographs of P92 and E911, as received

The particle dimensions were measured on the TEM micrographs taken from the extraction double replicas. The size of the coarse $M_{23}C_6$ was about 100 nm, while fine MX were about 20 nm in diameter. The mean diameter d of $M_{23}C_6$ in P92 was smaller (d=90 nm) than that in P91 (d=99 nm). The diameter of the fine MX particles which influence creep resistance of these steels was similar in P91 (d=16±7 nm) and P92 (d=22±12 nm). The V-wings in P92 have a length of major axis of 78 ± 15 nm; there were no V-wings present in P91.

Long term creep

Well developed sub-grains of low dislocation density in the interiors were characteristic features of long-term exposed specimens (Figure 4). Figure 5 shows the results of quantitative measurements of dislocation density and sub-grain width with increasing creep time for P92 specimens exposed at 600 and 650°C. It can be seen that the dislocation density decreases quickly from 7.8 to 2.5 x 10^{14} m^{-2} after about 5000 h exposure.

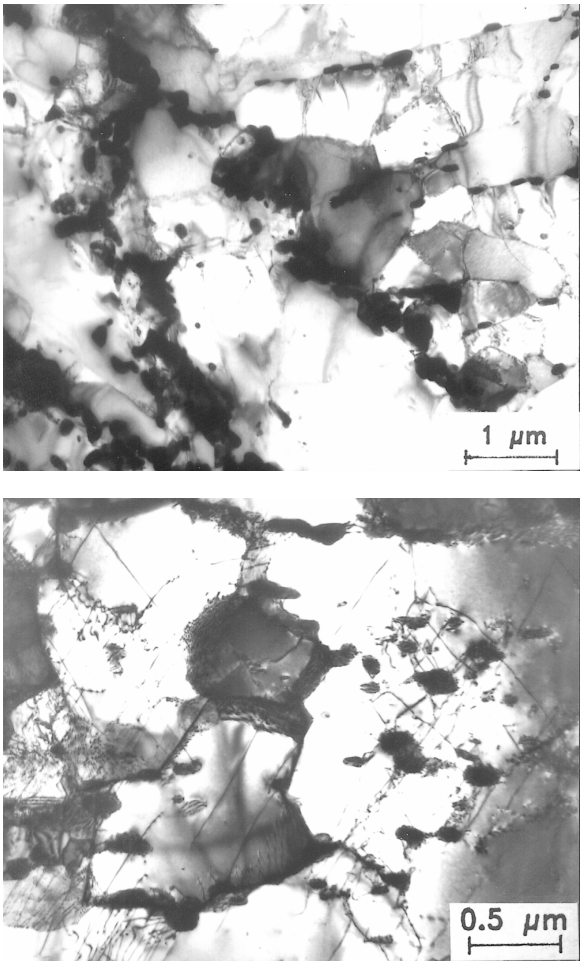

Fig. 4. TEM micrographs of P92 and E911 after creep deformation at 145 MPa / 600 ° C; P92 – 17 550 h, E911 – 17900 h

Comparison with the creep rate results shown in Figure 2 show that the rapid decrease in dislocation density is correlated with the region of the higher stress exponent. The prior austenite grain boundaries and subgrain boundaries were decorated by $M_{23}C_6$ carbides. Fine MX precipitates and the V-wings consisting of a NbX core and VN plates were observed inside the subgrains, Figure 6.

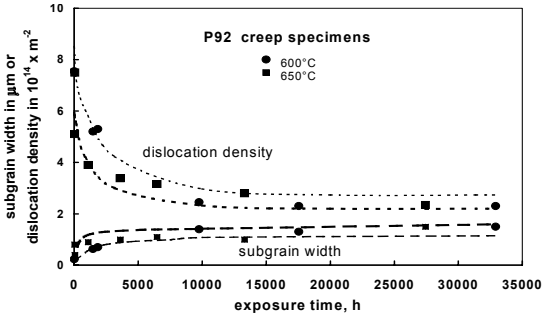

Fig. 5. Change in dislocation density and sub-grain width in steel P92 creep tested at 600 and 650°C

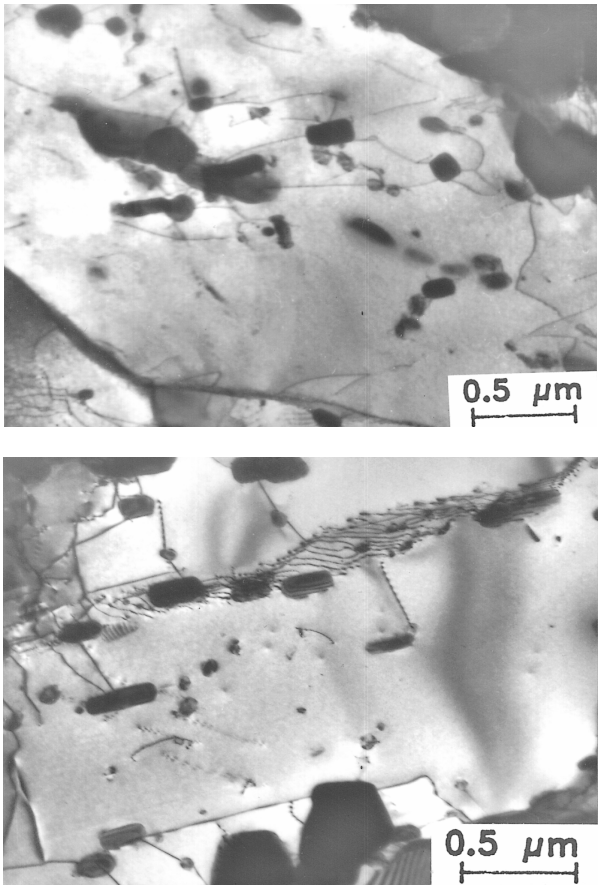

Fig. 6. TEM micrographs of P92 and E911 after creep deformation at 600 ° C; P92, 145 MPa, 33 000 h and E911, 132 MPa, 22 200 h

The $M_{23}C_6$ precipitates coarsened during creep testing but the MX remained essentially unchanged; the increases in mean carbide particle diameter of both $M_{23}C_6$ and MX with increasing exposure time at 600°C are shown in Figure 7. It should be noted that an applied stress appeared to accelerate the $M_{23}C_6$ coarsening process, the carbides in the unstressed head of the specimen being rather smaller than those in the stressed gauge portion of the specimen. Again this correlates with the high creep stress exponent region in Figure 2, the particle coarsening leading to higher creep rates than expected if only short-term data are considered. Similar microstructural evolution mechanisms caused by creep deformation of other 9-12% chromium steels have been described in [9-15].

Precipitation of the Laves phase $Fe_2(W,Mo)$ was observed in P92 and E911 specimens exposed at 600 and 650°C. Typical composition of the Laves phase in P92 (9755 h at 600°C specimen) in atom % was 48.7 Fe, 17.7 Cr, 28.5 W, 3.7 Mo and 1.3 V. This phase was precipitated as large particles usually associated with the $M_{23}C_6$ precipitates at the prior austenite grain boundaries, as shown in Figure 8. TEM-EDS analysis of the $M_{23}C_6$ particles showed that W was enriched in the carbide phase – the composition in atom % of the $M_{23}C_6$ in a P92 creep specimen tested for 9755 h at 600°C was found to be 28.2 Fe, 59.2 Cr, 9.9 W, 1.5 Mo and 1.2 V.

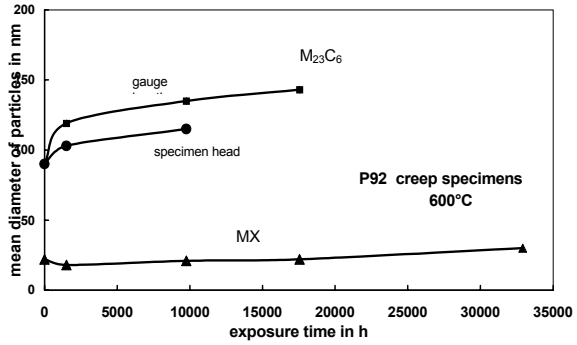

Fig. 7. Size of precipitates formed during creep exposure of P92 steel at 600°C

TEM-EDS analysis of the $M_{23}C_6$ particles showed that W was enriched in the carbide phase – the composition in atom % of the $M_{23}C_6$ in a P92 creep specimen tested for 9755 h at 600°C was found to be 28.2 Fe, 59.2 Cr, 9.9 W, 1.5 Mo and 1.2 V.

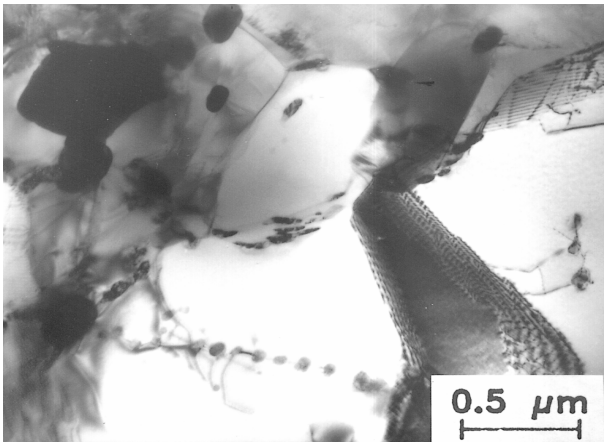

Fig. 8. Laves phase precipitate in a P92 creep specimen

It has been argued that the formation of Laves phase is detrimental because it removes the solid solution strengthening element W from the matrix to form particles which are so large that a strengthening effect by acting as effective barriers to dislocation motion cannot be expected. However, the presence of the phase at the sub-grain and prior austenite grain boundaries may stabilize these boundaries and prevent grain boundary sliding, a deformation mode which becomes increasingly important at low stresses. Furthermore, the Laves phase also removes Fe atoms form the matrix, so that the concentration of W in the Fe based matrix could remain essentially unchanged.

The creep strength of the steels examined increased with increasing W content (Figure 1) and the differences persisted to long test durations. The recovery of the martensite and associated decrease in dislocation density appeared to be slowed by the addition of W. The stress at which the secondary creep rate exponent n changed from 16 (high stress region dominated by the high dislocation density) to 6 (low stress region dominated by precipitation hardening) as the W content of the steel increased.

3.3. Oxidation behaviour

The development of the new Cr steels described in this report has been based on the achievement of high creep and stress rupture strength. At operating temperatures of 600°C and above, the oxidation resistance of the steels in steam and in flue gas can become a potentially life-limiting factor. It was shown in [5, 15] that in test atmospheres containing above a few percent by volume of water vapour, the protective, spinel-based oxide scales that form in dry air providing excellent resistance to oxidation cannot form. The rate of oxidation (weight gain) in atmospheres containing water vapour is a factor of about 30 higher than that observed in dry air. The further development of martensitic steels that can operate at temperatures of 600°C and above needs to address the steam oxidation problem and current developments, for example in the COST 522 and 536 Action [17], are examining new steel compositions designed for improved steam oxidation resistance.

4. Summary

The quantitative evaluation of the microstructure evolution in the steel P91, P92 and E911 steels showed that in the first 3000 h of exposure there was a rapid reduction in the dislocation density and an increase in the size of the $M_{23}C_6$ precipitates. The MX precipitates exhibited insignificant change in size.

The microstructural changes were reflected in the results of the creep tests and it is necessary to pay special attention to the microstructural evolution when extrapolating creep rupture data for these steels.

The high creep strength that has been achieved in the investigated steels enables them to be considered for applications in advanced power plants operating at steam temperatures above 600°C. However the 9% Cr steels do not possess adequate oxidation resistance for application as thin-walled components in steam-containing environments at temperatures above 600°C. Development efforts are now directed towards the higher chromium steels (10-12%) which have sufficient oxidation resistance while maintaining high creep rupture strength.

References

[1] V.K. Sikka, C.T. Ward and K.C. Thomas, in Ferritic Steelsfor High Temperature Applications, Warren, PA, USA, 6-18 October 1981, 65, ASM (1983).

[2] Nippon Steel Corporation, Data Package for NF616 Ferritic Steel, January 1993, second edition, March (1994).

[3] W.J. Quadakkers, P.J. Ennis, The oxidation behaviour of ferritic and austenitic steels in simulated power plant service environments, Proceedings of 6 Int. Conference on Materials for Advanced Power Engineering 1998, 5-7.10. 1998, Liège, Belgium, J.Lecomte-Beckers, F.Schubert, P.J.Ennis (eds.), ISBN 389336 228-2, Forschungszentrum Julich, 1998, 128-138.

[4] Summary of average stress rupture properties of wrought steels for boilers and pressure vessels, ISO Technical Report 7468, Ref. No. ISO/TR 7468-1981 (E), 1981.

[5] O. Wachter, P.J .Ennis, A. Czyrska-Filemonowicz, A. Zielińska-Lipiec, H. Nickel, Investigation of the properties of 9% Cr steel of the type 9Cr-0.5Mo-1.8W-V-Nb with respect to its application as a pipe work and boiler steel operating at elevated temperatures, Report of the Research Centre Jülich, Jül-3074, ISSN 0944-2952 (1995).

[6] P.J. Ennis, A. Zielinska-Lipiec, O. Wachter, A. Czyrska-Filemonowicz, Microstructural stability and creep rupture strength of Martensitic steel P92 for advanced power plant, Acta Materialia, 45, 4901 (1997).

[7] A. Zielinska-Lipiec, A. Czyrska-Filemonowicz, P.J. Ennis, O. Wachter, The influence of heat treatments on the microstructure of 9% chromium steels containing tungsten, Journal of Materials Processing Technology, 64 (1997) 397-405.

[8] F.Abe, T.Horiuchi, et al, Stabilization of the Martensitic microstructure in advanced 9Cr steel during creep at high temperature, Acta Materialia 378 (2004) 299-303.

[9] A. Zielińska-Lipiec, A. Czyrska-Filemonowicz, P.J. Ennis, Microstructure and creep behaviour of the new 9% Cr steel containing tungsten for power generation, Proceedings of the 4th International Scientific Conference "Achievements in Mechanical & Materials Engineering" AMME'95, Gliwice-Wisła, 1995, 363-366.

[10] A. Czyrska-Filemonowicz, P.J. Ennis, A. Zielińska-Lipiec, High chromium creep resistance steel for modern power plant application, Proceedings of the "Metallurgy on the Turn of 20th Century", K. Swiatkowski (ed.) Committee of Metallurgy, Kraków 2002, 193-219.

[11] J. Plesicka, R. Kuzel, A. Dranhofer, G. Egger; The evolution of dislocation density during heat treatment and creep of tempered martensite ferritic steels, Acta Materialia 51 (2003) 4847-4862.

[12] V. Sklenicka, K. Kucharowa, M. Svoboda, L. Kloc, J. Bursik, A. Kroupa, Long-term creep behaviour of 9–12%Cr power plant steels, Materials Characterisation; 51 (2003) 35-48.

[13] A. Hernas, G. Moskal, K. Rodak, J. Pasternak, Properties and microstructure of 12%Cr-W steels after long – term service, JAMME, 17 (2005) 69-72.

[14] A. Zielińska-Lipiec, A. Czyrska-Filemonowicz, P.J Ennis, Microstructure and creep behaviour of the 9%Cr steel containing Tungsten, Journal of Materials Processing Technology, 64 (1997) 397-405.

[15] D. Allen, B. Harvey, The influence of oxidation on long term creep rupture strength data, Proceedings of 8th Int. Conference on Materials for Advanced Power Engineering 2006, Liège, Belgium, J.Lecomte-Beckers, F.Schubert, P.J.Ennis (eds.), ISBN 389336 228-2, Forschungszentrum Julich, 2006, Part III, 1479-1490.